

## Joint density of states in interband transitions in semiconductors in a magnetic field

L. R. Ram Mohan

*Physics Department, Worcester Polytechnic Institute, Worcester, Massachusetts 01609*

Peter A. Wolff

*Francis Bitter National Magnet Laboratory, Massachusetts Institute of Technology,  
Cambridge, Massachusetts 02139*

(Received 12 August 1982)

We consider impurity collision broadening of electron and hole Landau levels in a magnetic field, and the effect of electron-hole correlated impurity scattering to all orders on the joint density of states of interband transitions in a semiconductor. These renormalization mechanisms eliminate the divergences in the density of states associated with the unperturbed states for electrons and holes at Landau levels. This calculation has relevance in several physical situations involving interband transitions in the presence of a magnetic field; in particular, we discuss the calculation of gain for stimulated plasmon emission by electron-hole recombination in narrow-band-gap semiconductors.

## I. INTRODUCTION

An applied magnetic field provides an effective, controlled, external perturbation for the study of electron energy levels in solids. The perturbing magnetic field alters the continuous electron levels in energy bands in a fundamental way due to Landau quantization. In the usual theory the level density displays characteristic infinite peaks at the positions of the Landau energy levels. These peaks manifest themselves as infinities in the joint density of states in intraband as well as interband transitions between magnetic levels in solids. In experimental magneto-optic absorption studies such transitions between magnetic levels appear as sharp peaks of finite height in the observed spectra. The line shapes have traditionally been parametrized with Lorentzian parameters and the theoretical representation of the infinite peak has been used essentially to determine the position of the peak and to identify it as arising from a specific transition.<sup>1</sup> A related problem is the evaluation of the gain in electron-hole recombination in a magnetic field. Without the removal of the divergence in the joint density of states one would be led to an infinite gain for a solid-state laser in a magnetic field. Thus an investigation of mechanisms which govern the line shapes and laser gain in magneto-optical transitions is of interest.

The first *ab initio* calculation of finite lifetimes for carriers in a magnetic field was carried out by Kubo *et al.*,<sup>2</sup> who were interested in galvanomagnetic effects and the Shubnikov-de Haas oscil-

lations of the magnetoresistance. An extension of Kubo's approach to investigate the line shapes in magnetoabsorption and interband transitions was made by Korovin and Kharitonov,<sup>3</sup> who evaluated level broadening effects from interactions with phonons. They calculated only renormalization effects for the self-energy of the electrons and holes, the "scattering out" terms in a kinetic equation formulation, and neglected vertex corrections which correspond to "scattering in" terms in the driving terms of the kinetic equation. Later, Sacks and Lax<sup>4</sup> studied the recombination process in semiconductors in a magnetic field and took account only of level broadening effects arising from interactions with impurities and phonons. Using this approach they evaluated the gain in the recombination process in semiconducting lasers operating in the presence of a magnetic field. With the level broadening included in the joint density of states they estimated the finite gain in semiconducting lasers. Their calculation was done without including vertex corrections.

In the present calculation we consider elastic scattering of electrons and holes with impurities as a mechanism for line broadening and the effect this has on interband transitions in narrow-gap semiconductors in high magnetic fields. The finite lifetimes of the quasiparticles arise from elastic collisions of these particles with impurities which are randomly distributed in the crystal. The random positioning of impurities introduces an irreversibility in the problem thereby providing damping for a quasiparticle wave packet. We use the diagram approach<sup>5</sup> to evaluate the self-energy, and consider correlated

electron-hole scattering off impurities to account for renormalization of the polarization bubble diagram. It is well known that the latter are the important driving terms associated with the scattering in effects in the kinetic equation approach.

The essential features of the impurity potential scattering are well represented by the exactly solvable model with a  $\delta$ -function potential of the form  $V_0\delta(\vec{r})$ . This approximation yields a level density for the  $n=0$  Landau level similar to that given by a Gaussian potential in the limit of high fields. The strength of the potential can be normalized to the actual scattering cross section by using experimental data on the mobilities of electrons and of holes. Under these conditions we are able to evaluate an infinite set of ladder diagrams in the renormalization of the polarization bubble. Our numerical studies (Sec. IV, below) show that the renormalization effects can be substantial.

In Sec. II we give a brief description of the problem and, for completeness, show the presence of the infinite density of states in interband transitions for each  $n$  in a magnetic field. In Sec. III, we present a diagrammatic calculation of the Green's function and the dielectric polarization.

## II. DIVERGENCE IN THE JOINT DENSITY OF STATES

Consider a very general situation in interband transitions in a direct-gap semiconductor in which we have a distribution of electrons in the conduction band and a quasithermal distribution of holes in the valence band maintained, for example, by optical pumping. This would permit us to study stimulated emission via electron-hole recombination as well as interband transitions in the intrinsic case. The typical intraband processes leading to thermalization of the carriers are at least an order of magnitude faster than the interband recombination rate,<sup>6</sup> assuming a steady pumping rate to maintain electron and hole number densities. We can then define quasi-Fermi-levels  $\mu_c$  and  $\mu_v$  for electrons and holes, respectively.<sup>7</sup> Ignoring the dependence on spin for the present, the energy spectrum is given by

$$E_{c,\alpha} = E_g + \frac{\hbar^2 k_z^2}{2m_c^*} + \hbar\omega_0(n + \frac{1}{2}), \quad \alpha = (n, k_y, k_z),$$

$$E_{v,\alpha} = -\frac{\hbar^2 k_z^2}{2m_v^*} - \hbar\omega_0(n + \frac{1}{2}).$$
(1)

Here  $\omega_0$  is the cyclotron frequency.

The wave functions for the electron, in Bloch's form, are given by

$$\Psi_{v,\alpha} = u_v(\vec{r}) \exp(ik_y y + ik_z z) h_n(x - l^2 k_y),$$

$$v = c, v$$
(2)

with  $h_n(x)$  being the normalized Hermite functions. The Green's function for the electrons can be written as

$$G(\vec{x}, \vec{x}', \omega) = \hbar \sum_{v,\alpha} \Psi_{v,\alpha}(\vec{x}) \mathcal{G}_v(\omega, E_{v,\alpha}) \Psi_{v,\alpha}^*(\vec{x}')$$
(3)

with

$$\mathcal{G}_v(\omega, E_{v\alpha}) = \frac{1 - f(\mu_v, E_{v\alpha})}{\hbar\omega - E_{v\alpha} + i\delta} + \frac{f(\mu_v, E_{v\alpha})}{\hbar\omega - E_{v\alpha} - i\delta},$$
(4)

where  $f$  is the Fermi function.

Let us display the divergence in the density of states for each  $n$ . The number density  $n_v$  of carriers can be expressed, with an appropriately chosen contour, as

$$n_v = -i \lim_{\delta \rightarrow 0} 2 \int \frac{d\omega}{2\pi} e^{i\omega\delta} G(\vec{x}, \vec{x}, \omega)$$

$$= 2 \sum_n \int \frac{dk_y dk_z}{(2\pi)^2} [h_n(x - k_y l^2)]^2 f(\mu_v, E_{v\alpha})$$

$$= \int_0^{\mu_v} dE \rho(E).$$

The factor of 2 arises from spin degeneracy.

The level density  $\rho(E)$  is given by

$$\rho(E) = \frac{2}{(2\pi l)^2} \left[ \frac{2m_v}{\hbar^2} \right]^{1/2} \sum_n (E - E_{v\alpha})^{-1/2}$$
(5)

with the expected divergent behavior at the Landau levels  $E = E_{v\alpha}(k_z = 0)$ .

We now consider the contribution of the interband transitions to the dielectric function

$$\epsilon(\omega, \vec{q}) = \epsilon_\infty - (4\pi/q^2) \Pi(\omega, \vec{q}),$$
(6)

where  $\epsilon_\infty$  is the high-frequency dielectric constant. Representing the polarization  $\Pi$  in terms of Green's functions we have

$$\Pi(x, x', t - t') = -i(e^2/\hbar) 2G(x, x', t - t')$$

$$\times G(x', x, t' - t),$$

and

$$\Pi(\omega, \vec{q}) = 2e^2 \sum_{\nu'} \sum_n \int \frac{dp_z}{(2\pi l)^2} \int \frac{dp_0}{2\pi i \hbar} |M_{\nu\nu'}(\vec{q})|^2 \mathcal{G}_{\nu}(p_0, E_{\nu n}(p_z)) \mathcal{G}_{\nu'}(p_0 + q_0, E_{\nu n}(p_z + q_z)). \quad (7)$$

For interband transitions the usual selection rules  $\Delta n = 0$ ,  $\Delta \vec{q} = 0$  apply so that the transition matrix element at the band edge can be considered to be representative of its behavior over the available range of momenta. We then have

$$(4\pi/q^2)\Pi(\omega, \vec{q}=0) = (e^2/q^2) |M_{cv}(\vec{q})|^2 \sum_n \int \frac{dp_z}{(2\pi l)^2} (f_c - f_v) \left[ \frac{1}{(E_{c\alpha} - E_{v\alpha} + \hbar q_0)} - \frac{1}{(E_{c\alpha} - E_{v\alpha} - \hbar q_0)} \right], \quad (8)$$

with the joint density of states given by

$$\rho(E, \omega, \vec{q}=0) = (4\pi e^2 |M_{cv}(\vec{q})|^2 / q^2) \sum_n \int \frac{dp_z}{(2\pi l)^2} (f_c - f_v) \delta(E - E_{c\alpha} + E_{v\alpha}).$$

Setting

$$1/\bar{m} = (1/m_c^*) + (1/m_v^*)$$

we have

$$\rho(E, \omega, \vec{q}=0) = [4\pi e^2 |M_{cv}(\vec{q})|^2 / q^2] \frac{1}{(2\pi l)^2} \left[ \frac{2\bar{m}}{\hbar^2} \right]^{1/2} (f_c - f_v) [E - E_g - 2\hbar\omega_0(n + \frac{1}{2})]^{-1/2}, \quad (9)$$

again showing the divergent behavior for energies matching the difference between the Landau levels in the conduction and valence bands.

The singular behavior of the level density (5) and the joint density of states (9) is washed out by a broadening of the energy levels. Physically, the level broadening occurs as follows. In high magnetic fields the electron (or hole) wave packet is elongated in the direction of the field. In the situation where the number density of impurities  $n_s$  is such that  $n_s^{-1/3} \gg l$  the electron encounters fewer scatterers in the direction perpendicular to the field, than in the direction of the field, in the time scales of the order of  $\omega_0^{-1}$ . This consideration makes the scattering problem essentially one dimensional along the direction of the field. Since the electron wave function overlaps many scatterers, an electron which scatters off an impurity is likely to encounter many other scatterers in its motion along the field before reencountering the first impurity. This is taken into account, as was done by Kubo *et al.*, in the self-consistent evaluation of the self-energy to all orders in perturbation theory. Furthermore, the joint density of states is modified by the vertex corrections. The electron-hole pair is created at the same space-

time point and they both have similar envelope wave functions due to the  $\Delta n = 0$  selection rule in the interband transition. This implies that they interact with the same scatterers. The effect of this correlated scattering off impurities can be taken account of to all orders in the ladder approximation as shown in the following section.

### III. DIAGRAMMATIC CALCULATION OF THE GREEN'S FUNCTIONS

In the extreme quantum limit the carriers occupy the  $n = 0$  Landau level with specific spin polarizations in the conduction and valence bands. With the spin magnetic energy in the external field included in the energy gap, we have the energy spectrum

$$\begin{aligned} E_{c\alpha} &= E_{cn=0}(k_z) = E_g + \hbar^2 k_z^2 / 2m_c^*, \\ E_{v\alpha} &= E_{vn=0}(k_z) = -\hbar^2 k_z^2 / 2m_v^*. \end{aligned} \quad (10)$$

The interaction Hamiltonian density for the potential scattering is assumed to be

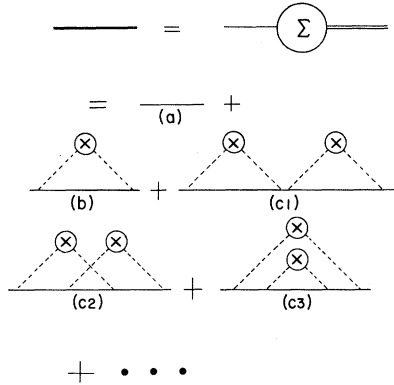


FIG. 1. Perturbation series for the propagator. Here  $\Sigma$  is the self-energy. Dashed lines represent the impurity potential.

$$H_{\text{int}}(\vec{r}, t) = \sum_{i=1}^{n_s} \Psi^*(\vec{r}, t) V_0 \delta(\vec{r} - \vec{R}_i) \Psi(\vec{r}, t), \tag{11}$$

where  $\vec{R}_i$  are the positions of the randomly distributed impurities. The potential strength  $V_{0c}$  (or  $V_{0v}$ ) for electrons (holes) can be related to their mobilities  $\mu = e\tau/m^*$ , since the collision frequency is expressible as

$$1/\tau = n_s \langle v_f \rangle 4\pi(m^* V_0 / 2\pi\hbar^2)^2, \tag{12}$$

where  $\langle v_f \rangle$  is the average velocity for the Fermi distribution. The experimentally determined mobilities thus normalize the potential strength.

The full set of diagrams for the electron propagator after averaging over the impurity positions is represented by Fig. 1. The self-consistent treatment of the self-energy consists of evaluating the sum of the diagrams in Fig. 2 with the series of nested self-energy insertions. The diagrams of the type Fig. 1(c2) with crossed legs for the potential are numerically smaller than those without crossings and

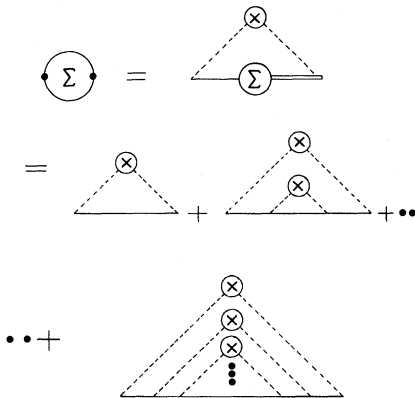


FIG. 2. Diagrams for the self-consistent determination of the self-energy.

are neglected. Also, the dominant contribution will be from the  $n=0$  intermediate states since the higher  $n$  states will be much higher in energy in high magnetic fields. In this limit the Kubo form of the self-energy obtains. The self-energy here is a function only of energy and we have

$$\Sigma_\nu(p_0) = \frac{|V_0|^2 n_s}{(2\pi l)^2 \hbar} \int dp_z \frac{1}{\hbar p_0 - E_{v n=0}(p_z) - \Sigma_\nu(p_0)}, \tag{13}$$

$\nu = c, v.$

After performing the  $p_z$  integral we find

$$\Sigma_c(p_0) = (2\pi i) \frac{|V_{0c}|^2 n_s}{(2\pi l)^2 \hbar} \left[ \frac{m}{2} \right]^{1/2} \times \frac{1}{[p_0 - E_g - \Sigma_c(p_0)]^{1/2}}, \tag{14}$$

$$\Sigma_v(p_0) = -(2\pi i) \frac{|V_{0v}|^2 n_s}{(2\pi l)^2 \hbar} \left[ \frac{m_v^*}{2} \right]^{1/2} \times \frac{1}{[\Sigma_v(p_0) - p_0]^{1/2}}. \tag{15}$$

The roots of the cubic equations (14) and (15) are determined for obtaining the self-energies. The root corresponding to  $\text{Im}\Sigma_c \geq 0$  for  $p_0 \geq \mu_c$  and  $\text{Im}\Sigma_v \geq 0$  for  $p_0 \geq \mu_v$  is chosen as the physically allowed one.

The modified density of states is obtained on noting that the number density is

$$n_\nu = \int \frac{dp}{(2\pi l)^2} f(\mu_\nu, E_{\nu\alpha}) = \text{Re} \int \frac{dE}{(2\pi l)^2} \left[ \frac{2m^*}{\hbar^2} \right]^{1/2} f(\mu_\nu, E_{\nu\alpha}) \times \frac{1}{[E - E_\nu(p_z=0) - \Sigma^*]^{1/2}}, \tag{16}$$

so that

$$\rho_\nu(E) = (1/\pi N_s |V_0|^2) \text{Im}\Sigma_\nu(E). \tag{17}$$

Here (17) follows from (14) or (15). For typical values of the mobility (of  $10^4 - 10^5$  cm<sup>2</sup>/V sec) the density of states in the  $n=0$  levels in the conduction and valence bands is shown in Fig. 3. The interactions with the randomly sited impurities thus eliminate the infinity in the density of states.

We now turn to the renormalization of the polarization bubble graph. From (7) we have in the extreme quantum limit

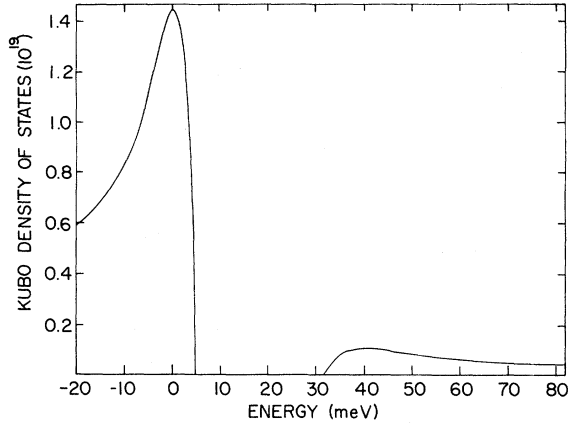


FIG. 3. Density of states in the conduction and valence bands for the  $n=0$  level after impurity broadening in  $\text{Hg}_{1-x}\text{Cd}_x\text{Te}$  for electron concentration of  $10^{17}/\text{cm}^3$  and hole concentration of  $10^{15}/\text{cm}^3$  at 65 kG.

$$(4\pi/q^2)\Pi(\omega, \vec{q}) = (4\pi e^2/q^2) |M_{cv}(\vec{q})|^2 \times D(\omega, \vec{q}). \quad (18)$$

With no vertex corrections we have

$$D^0(\omega, \vec{q}) = \int \frac{dp_0}{(2\pi i)} \int \frac{dp_z}{(2\pi l)^2 \hbar} \mathcal{G}(p_0, E(p_z)) \times \mathcal{G}(p_0 + \omega, E(p_z + q_z)) \quad (19)$$

with  $\mathcal{G}$  given by (4). Here we have dropped a spin

$$D(\omega, \vec{q}=0) = \int \frac{dp_0}{(2\pi i)} [P(p_0, \omega) + P(p_0, \omega)(n_s V_{0v} V_{0c})P(p_0, \omega) + \dots], \\ = \int \frac{dp_0}{(2\pi i)} \frac{P(p_0, \omega)}{1 - n_s V_{0v} V_{0c} P(p_0, \omega)}, \quad (21)$$

where

$$P(p_0, \omega) = \int \frac{dp_z}{(2\pi l)^2 \hbar} \mathcal{G}(p_0, p_z) \mathcal{G}(p_0 + \omega, p_z). \quad (22)$$

In view of the complicated dependence of  $\Sigma$  on  $p_0$  the energy integral cannot be performed immediately even for the lowest-order term (19); on the other hand, contour integration over  $p_z$  leads to four terms, two each for the excitation and the deexcitation of the electron across the band gap. Introducing the notation

$$\sigma = m_v^*/m_c^*, \\ r = |V_{0v}/V_{0c}|^2,$$

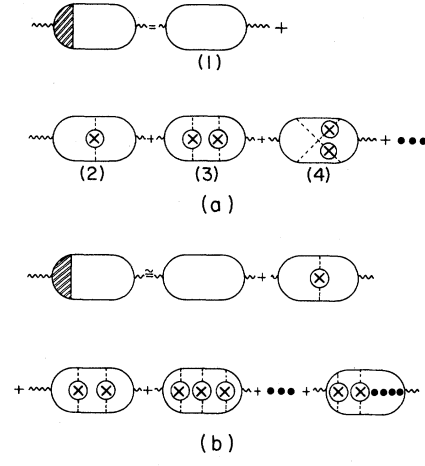


FIG. 4. (a) Polarization diagrams with vertex corrections. (b) Ladder approximation to the renormalization of the vertex.

factor of 2 since we are concerned with energy levels of specific spin polarization. The propagators  $\mathcal{G}$  are the renormalized ones with

$$\mathcal{G}^{-1} = \mathcal{G}_0^{-1} - \Sigma(p_0). \quad (20)$$

The vertex renormalization diagrams are shown in Fig. 4(a). In the extreme quantum limit the contribution of diagrams with crossed rungs, as in diagram (4) of Fig. 4(a), can be shown to be numerically smaller than those with no crossing of the potential lines. In the ladder approximation represented by Fig. 4(b), we find that the vertex renormalization terms constitute a geometric series so that

$$N_1 = \sigma r \Sigma_c^*(p_0) + \Sigma_v(p_0 + \omega), \\ N_2 = \sigma r \Sigma_c^*(p_0 + \omega) + \Sigma_v(p_0), \quad (23)$$

$$D_1 = (1 + \sigma)p_0 + \sigma\omega - E_g - \Sigma_c^*(p_0) \\ - \sigma \Sigma_v(p_0 + \omega), \\ D_2 = (1 + \sigma)p_0 + \omega - E_g - \Sigma_c^*(p_0 + \omega) \\ - \sigma \Sigma_v(p_0),$$

we have

$$P(p_0, \omega) = (|V_v|^2 n_s)^{-1} \{ f_c(p_0)[1 - f_v(p_0 + \omega)](N_1/D_1) + f_c(p_0 + \omega)[1 - f_v(p_0)](N_2/D_2) \\ + [1 - f_c(p_0)]f_v(p_0 + \omega)(N_1^*/D_1^*) + [1 - f_c(p_0 + \omega)]f_v(p_0)(N_2^*/D_2^*) \}. \quad (24)$$

Further progress requires numerical integration over  $p_0$  after substituting (24) in (21), and the consideration of specific processes. In the case of an intrinsic semiconductor we would set  $f_v = 1$  and  $f_c = 0$  to obtain the dielectric response corresponding to interband absorption.

In order to bring out the physically interesting features in a specific case, we study in detail the recombination of electrons with holes across the band gap and calculate the gain in the emission mode associated with electron-hole recombination for an inverted population. Such a case is realized in the consideration of a solid-state laser operating in a magnetic field in which electrons are pumped from the valence band to above the Fermi level in the conduction band, optically or by using an electron beam, to create the inverted population. The recombination of the electrons from the bottom of the conduction band with holes across a direct gap leads to emission of radiation farther in the infrared region from the pump frequency.

While the narrow band-gap materials may be considered to be ideal for the generation of stimulated emission of radiation in the far infrared region of wavelengths greater than  $20 \mu\text{m}$ , they have the following limitation. As soon as the band gap matches the energy of an internal mode of the material, such as LO phonons or plasmons associated with the collective modes of the carriers, the carrier lifetime drops to the picosecond range. This makes the stimulated emission of photons less favorable in comparison with the dissipation of energy from the recombination of electrons and holes into these modes. Recently,<sup>8</sup> it was suggested that this seeming disadvantage can be turned in our favor by generating, in the confined geometry of thin films, the stimulated emission of plasmons which can then be converted to radiation at the surface of the material. The numerical results described in Sec. IV include the effect of plasmons and are for the recombination process in  $\text{Hg}_{1-x}\text{Cd}_x\text{Te}$  in a magnetic field.

#### IV. NUMERICAL RESULTS

We consider  $n\text{-Hg}_{1-x}\text{Cd}_x\text{Te}$  in the semimetallic regime with  $x=0.13$ . For such a material we have shown<sup>8</sup> that the pumping rate for stimulated emission of plasmons is minimized. In a large magnetic field this zero-gap material develops a field-induced

gap between the conduction and valence bands. For carrier concentrations of  $10^{17}/\text{cm}^3$  electrons, the plasmon energy  $\hbar\omega_p$  matches the bandgap for magnetic fields of the order of 60 kG. An exact resonance matching for the emission of plasmons can be achieved by the simple device of varying the magnetic field. We evaluate the gain for the stimulated emission of plasmons under such conditions.

Using an electron mobility of  $10^5 \text{ cm}^2/\text{V sec}$  and a hole mobility of  $10^3 - 10^4 \text{ cm}^2/\text{V sec}$  we evaluate the scattering potential strengths  $V_{0c}$  and  $V_{0v}$  using (12). The self-energies  $\Sigma_c$  and  $\Sigma_v$  are then solved from (14) and (15). The Kubo density of states for the  $n=0$  state in the valence and the conduction bands are as in Fig. 3. The level broadening arising from impurity scattering leads to the removal of the Landau singularity in the density of states and to the encroaching of the density of states into the band gap. The integration of (21) can be performed numerically to obtain the dielectric function

$$\epsilon(\omega, \vec{q}=0) = \epsilon_\infty (1 - \omega_p^2/\omega^2) \\ - \lim_{\vec{q} \rightarrow 0} (4\pi e^2/q^2) |M_{cv}(\vec{q})|^2 D(\omega, 0). \quad (25)$$

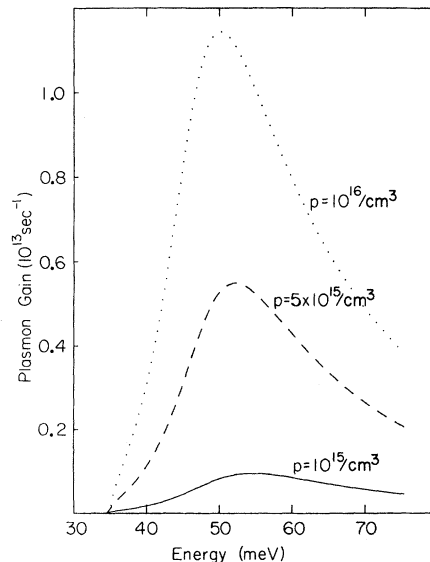


FIG. 5. Plasmon gain as a function of energy, for different hole concentrations, in  $\text{Hg}_{1-x}\text{Cd}_x\text{Te}$  at 65 kG. Hole mobility is  $10^4 \text{ cm}^2/\text{V sec}$ .

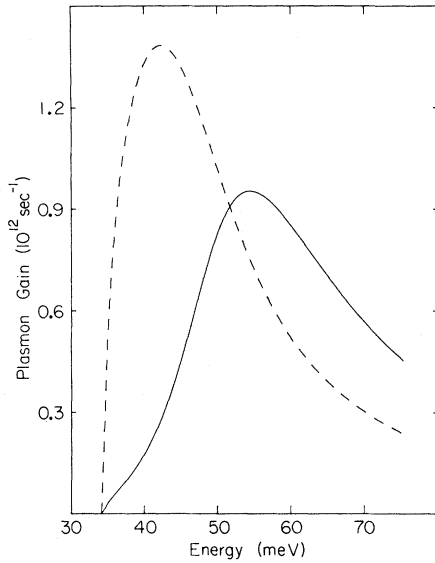


FIG. 6. Effect of vertex renormalization on the plasmon gain. Full curve represents the laser gain with the vertex corrections and the dotted curve the effect of neglecting these contributions, for a hole concentration of  $10^{15}/\text{cm}^3$ .

The plasmon gain is then given by

$$\Gamma = (\omega_p / 2\epsilon_\infty) \text{Im}\epsilon(\omega, \vec{q}=0). \quad (26)$$

The behavior of the gain as a function of frequency is shown in Fig. 5.

The gain increases with increasing hole concentration and estimates show that the gain exceeds the plasmon damping by about a factor of 2 for hole concentrations of  $5 \times 10^{15}/\text{cm}^3$ . In Fig. 6 we compare the effect of including the vertex renormalization on the plasmon gain with the effect of not including the infinite set of ladder diagrams. The gain is reduced by these terms by about an order of magnitude.

Finally, we present in Fig. 7 the effect of temperature on the gain. The results displayed are obtained by using the full temperature-dependent Fermi distribution functions in (21). The curves in Fig. 7 show the weakening of the stimulated plasmon mode as the temperature is increased. At each temperature and carrier concentration the Fermi levels of electrons and of holes are determined in a self-consistent manner numerically using (16).

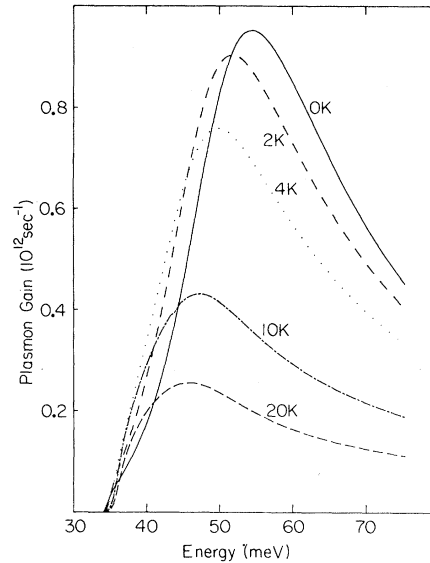


FIG. 7. Temperature dependence of the plasmon gain at  $B = 65 \text{ kG}$ .

## V. CONCLUSIONS

We have presented a general approach to the problems of line shape and of laser gain for the interband transitions in narrow-gap semiconductors in high magnetic fields, and provided a numerical study of the dielectric function in the situation with an inverted population leading to electron-hole recombination. The importance of the ladder diagrams in the polarization bubble has been demonstrated by quantitative numerical work. As mentioned before, these terms represent the scattering in terms in a kinetic formulation of the Boltzmann transport equation in the present case. We have found that the difference between including these terms and not including them gets more pronounced as the number density of carriers is increased.

Problems for further study are the effect on line shapes of phonon scattering, and the complete evaluation of the dielectric function in the intrinsic case, and the inclusion of more Landau levels in the analysis for somewhat lower magnetic fields than those considered here.

## ACKNOWLEDGMENT

This work was supported by AFOSR Contract No. F49620-80-C-008.

- <sup>1</sup>For reviews see, for example, B. Lax and J. G. Mavroides, in *Solid State Physics*, edited by H. Ehrenreich, F. Seitz, and D. Turnbull (Academic, New York, 1960), Vol. 11, p. 261; R. L. Aggarwal, in *Semiconductors and Semimetals*, edited by A. C. Beer and R. K. Willardson (Academic, New York 1972), Vol. 9, p. 151; M. H. Weiler, in *Semiconductors and Semimetals* (Academic, New York, 1981), Vol. 16, p. 119.
- <sup>2</sup>R. Kubo, S. J. Miyake, and N. Hashitsume, in *Solid State Physics* (Academic, New York, 1965), Vol. 17.
- <sup>3</sup>L. I. Korovin and E. V. Kharitonov, *Fiz. Tverd. Tela* (Leningrad) 7, 2162 (1965) [*Sov. Phys.—Solid State* 7, 1740 (1966)].
- <sup>4</sup>B. Sacks and B. Lax, *IEEE J. Quantum Electron.* 2, 607 (1966).
- <sup>5</sup>A. A. Abrikosov, L. P. Gorkov, and I. E. Dzyaloshinski, *Methods of Quantum Field Theory in Statistical Physics* (Prentice-Hall, Englewood Cliffs, New Jersey, 1963), Chap. VII.
- <sup>6</sup>P. A. Wolff, *Phys. Rev. Lett.* 24, 266 (1970); in *Proceedings of the Conference on the Physics of Semimetals and Narrow Gap Semiconductors*, edited by D. L. Carter and R. T. Bate (Pergamon, New York, 1971); D. A. Cammack, A. W. Nurmikko, G. W. Pratt, and J. R. Lowney, *J. Appl. Phys.* 46, 3965 (1975); A. Elci, *Phys. Rev. B* 16, 5443 (1977); R. Dornhaus and G. Nimtz, in *Proceedings of the International Conference on Recombination Semiconductors*, Southampton, 1978 (unpublished).
- <sup>7</sup>M. G. A. Bernard and B. Douraffourg, *Phys. Status Solidi* 1, 699 (1961).
- <sup>8</sup>P. A. Wolff, C. Verie, S. Yuen, M. E. Weiler, and L. R. Ram Mohan, in *Proceedings of the International Conference on Physics of Narrow Gap Semiconductors, Linz, 1981*, edited by E. Gornick, H. Henrich, and L. Palmetshofer (Springer, Berlin, 1982), p. 135.